

Band crossing in isovalent semiconductor alloys with large size mismatch: First-principles calculations of the electronic structure of Bi and N incorporated GaAs

Hui-Xiong Deng, Jingbo Li,* Shu-Shen Li, Haowei Peng, and Jian-Bai Xia

State Key Laboratory for Superlattices and Microstructures, Institute of Semiconductors, Chinese Academy of Sciences, P.O. Box 912, Beijing 100083, China

Lin-Wang Wang

Computational Research Division, Lawrence Berkeley National Laboratory, Berkeley, California 94720, USA

Su-Huai Wei

National Renewable Energy Laboratory, Golden, Colorado 80401, USA

(Received 4 August 2010; revised manuscript received 20 September 2010; published 17 November 2010)

For large size- and chemical-mismatched isovalent semiconductor alloys, such as N and Bi substitution on As sites in GaAs, isovalent defect levels or defect bands are introduced. The evolution of the defect states as a function of the alloy concentration is usually described by the popular phenomenological band anticrossing (BAC) model. Using first-principles band-structure calculations we show that at the impurity limit the N-(Bi)-induced impurity level is above (below) the conduction- (valence-) band edge of GaAs. These trends reverse at high concentration, i.e., the conduction-band edge of $\text{GaAs}_{1-x}\text{N}_x$ becomes an N-derived state and the valence-band edge of $\text{GaAs}_{1-x}\text{Bi}_x$ becomes a Bi-derived state, as expected from their band characters. We show that this band crossing phenomenon cannot be described by the popular BAC model but can be naturally explained by a simple band broadening picture.

DOI: [10.1103/PhysRevB.82.193204](https://doi.org/10.1103/PhysRevB.82.193204)

PACS number(s): 71.55.Eq, 71.20.Nr, 71.23.An

Mixing isovalent compounds AC with BC to form semiconductor alloys $A_{1-x}B_xC$ has been an effective way in band structure engineering to enhance the availability of material properties.¹⁻⁵ In most cases, the mixed isovalent atoms A and B , such as Al and Ga in $\text{Al}_{1-x}\text{Ga}_x\text{As}$ or As and Sb in $\text{GaAs}_{1-x}\text{Sb}_x$ are similar in their atomic sizes and chemical potentials; therefore, the physical properties of $A_{1-x}B_xC$ change smoothly from AC to BC , often with a small amount of bowing.^{4,5} However, in some cases when the chemical and size differences between the isovalent atoms A and B are large, adding a small amount of B to AC or vice versa can lead to a discontinuous change in the electronic band structure as reflected by the formation of isovalent defect levels near the band edges.^{2,3,6} These large size- and chemical-mismatched (LSCM) systems often show unusual and abrupt changes in the alloys' material properties,⁷⁻¹² which provide great potential in material design for novel device applications. For example, unusually large band gap bowing was observed in $\text{Ge}_{1-x}\text{Sn}_x$ (Refs. 7 and 8) and in $\text{GaAs}_{1-x}\text{N}_x$.^{9,10,13} For $\text{GaAs}_{1-x}\text{N}_x$, the band gap bowing is so large that adding N into GaAs can simultaneously lower its band gap and its lattice constant;^{9,10} for $\text{ZnTe}_{1-x}\text{O}_x$, intermediate band inside the band gap was observed, which made this alloy a strong candidate for high efficiency solar cell^{14,15} and thermoelectric power generations.¹⁶

Since the discovery of the isovalent defect levels for semiconductors in the 1960s,² many studies have been done to understand the formation mechanism and calculate the position of the isovalent-bound states. It is usually expected that when the electronegativity of the substitutional isovalent atom is much larger than the host atom, e.g., an N substitution in GaP and an O substitution in ZnTe, the isovalent defect level will form *below* the conduction-band minimum (CBM)

by pulling down the conduction-band-derived states, whereas when the electronegativity of the substitutional isovalent atom is much smaller than the host atom, e.g., an As substitution in GaN, or a Te substitution in ZnS, the isovalent impurity level will form *above* the valence-band maximum (VBM) by shifting up valence-band-derived states. However, there could be exceptions when strain plays important role.¹⁷⁻²⁰ For example, absorption and photoluminescence excitation measurements show that in dilute N-doped GaAs the strongly localized isolated nitrogen-impurity level exists at about 180 meV *above* the CBM,¹⁹ despite the fact that the N $2s$ orbital energy is much lower than the replaced As $4s$ orbital energy (Table I). Similar experimental studies have also shown that in dilute Bi doped GaAs the strongly localized isolated Bi-impurity level exists at about 100 meV *below* the VBM,²⁰ despite the fact that the Bi $6p$ orbital energy is much higher than the replaced As $4p$ orbital energy (Table I).

To understand how the impurity levels evolve when the alloy concentration x increases from impurity limit to finite value, Walukiewicz and co-workers^{22,23} first proposed the phenomenological two-level band anticrossing (BAC) model

TABLE I. The calculated s and p valence atomic orbital energies (in eV) of N, As, and Bi in ns^2np^3 configurations, respectively. The last column gives the Phillips' covalent radii (in Å) for these atoms (Refs. 18 and 21).

Atom	s	p	Ionic radius
N ($2s^22p^3$)	-18.414	-7.235	0.719
As ($4s^24p^3$)	-14.702	-5.345	1.225
Bi ($6s^26p^3$)	-14.742	-4.774	1.518

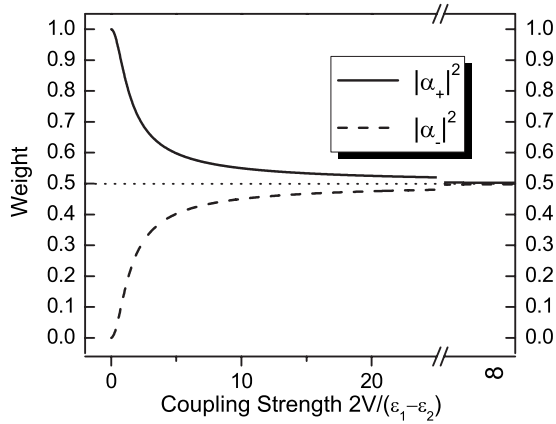


FIG. 1. The calculated weights $|\alpha_+|^2$ (solid line) and $|\alpha_-|^2$ (dashed line) of the upper and lower subbands, respectively, projected on the ϕ_1 state, based on the BAC model as a function of the relative coupling strength $2V/(\epsilon_1 - \epsilon_2)$.

to explain the pressure and composition dependencies of the band gaps of $\text{In}_y\text{Ga}_{1-y}\text{As}_{1-x}\text{N}_x$ alloys. Since then, this model has been extended to explain the band structures of other LSCM group IV, III-V, and II-VI alloys.^{7,24–26} The main feature of the BAC model is that the incorporation of an isovalent impurity will introduce a localized defect state close to the band edge. The coupling between the localized impurity state and the extended host band-edge state through a quantum anticrossing interaction produces two energy levels E_- and E_+ with the downward movement of the former near the conduction-band edge and the upward shift of the latter near the valence-band edge, leading to the band gap bowing observed in these LSCM alloys.^{22,24–26} More specifically, according to this BAC model, if the original states have energies ϵ_1 and ϵ_2 with wave function character ϕ_1 and ϕ_2 (assumed $\epsilon_1 > \epsilon_2$), then after the coupling with a coupling strength $V(x)$, which is assumed to be proportional to concentration x , the pair of energy levels E_- and E_+ will be

$$E_{\pm} = \frac{\epsilon_1 + \epsilon_2}{2} \pm \sqrt{\left(\frac{\epsilon_1 - \epsilon_2}{2}\right)^2 + V^2} \quad (1)$$

and the hybridized wave function can be expanded as

$$\psi_{\pm} = \alpha_{\pm}\phi_1 + \beta_{\pm}\phi_2. \quad (2)$$

Figure 1 shows the trends of coefficients $|\alpha_+|^2$ and $|\alpha_-|^2$ as a function of the relative coupling strength $2V/(\epsilon_1 - \epsilon_2)$. $|\beta_i|^2$ can be obtained using $|\beta_i|^2 = 1 - |\alpha_i|^2$. It is clear that the coefficient $|\alpha_+|^2$ of the upper subband after coupling is always larger than 0.5, i.e., the upper subband should always be a mostly ϕ_1 -like state, whereas $|\alpha_-|^2$ of the lower subband is always smaller than 0.5, so the lower subband should be a mostly ϕ_2 -like state, regardless how large the coupling strength V is. Taking the $\text{GaAs}_{1-x}\text{N}_x$ system as an example because the N_{As} impurity defect level is above the CBM of the host GaAs, then following the BAC model, the CBM of $\text{GaAs}_{1-x}\text{N}_x$ should always be derived mostly from the host GaAs CBM state. Similarly, for $\text{GaAs}_{1-x}\text{Bi}_x$, because its impurity defect level Bi_{As} is below the VBM of GaAs, then following the BAC model, the VBM of $\text{GaAs}_{1-x}\text{Bi}_x$ should

always be derived mostly from the host GaAs VBM state. However, previous direct first-principles density-functional-theory calculations^{9,18,27} and empirical potential calculations^{28–30} have shown that this expectation is not true when the impurity concentrations increase. Band crossing is observed at high concentration and is often interpreted as resulting from the formation of the N clusters.^{28–30}

In this paper, to check the validity of the popular BAC model and understand how the defect energy levels evolve in LSCM alloys, we present a systematic investigation on the electronic structure of $\text{GaAs}_{1-x}\text{Bi}_x$ and $\text{GaAs}_{1-x}\text{N}_x$ alloys, respectively, as a function of alloy concentration x . In our study, the dopants are introduced uniformly in the host and no nearest-neighbor impurity clusters exist. We find that for $\text{GaAs}_{1-x}\text{Bi}_x$ in the impurity limit, the Bi-derived impurity t_2 state is below the VBM, in agreement with experiment observation.²⁰ Similarly, for $\text{GaAs}_{1-x}\text{N}_x$ in the impurity limit, the N-derived impurity a_1 state is above the CBM, again in agreement with experimental observation.¹⁹ However, when the concentration x increases, the defect band widths increase, and eventually, the Bi- and N-derived energy levels become the top of the occupied valence state above the VBM of GaAs in $\text{GaAs}_{1-x}\text{Bi}_x$, or bottom of the unoccupied conduction band below the CBM of GaAs in $\text{GaAs}_{1-x}\text{N}_x$, respectively. The switching of the order between impuritylike levels and band-edge states at higher concentration is in line with the general expectation from the chemical trends of these elements (Table I) and can be explained by a simple band broadening model but it contradicts the description of the BAC model.

In this study the band-structure and total energy calculations are performed using the frozen-core projector-augmented wave method³¹ within the local density approximation (LDA) as implemented in the Vienna *ab initio* simulation package (VASP).³² Convergence with respect to the plane-wave cut-off energy has been checked. The Monkhorst-Pack method³³ is used to sample the k -point mesh in the Brillouin zone. All the atoms are allowed to relax until the quantum mechanical forces acting on each atom become less than 0.02 eV/Å. The calculated band gap of GaAs is 0.3 eV, smaller than the experiment band gap of 1.5 eV due to the well-known LDA band-gap error. In this paper, as we are only concerned with relative positions of the impurity level and the band edges as a function of alloy concentration, the LDA band-gap error will not affect qualitatively the physical phenomenon discussed in this Brief Report.

To identify the position of the isovalent defect level induced by Bi and N in GaAs relative to the band edges, we first calculate the partial density of states (PDOS) and define the center of the band as the weighted energy average

$$E_{\sigma}^{\alpha} = \frac{\sum_i E_i D_{\sigma}^{\alpha}(E_i)}{\sum_i D_{\sigma}^{\alpha}(E_i)}, \quad (3)$$

where $D_{\sigma}^{\alpha}(E_i)$ denotes the PDOS for σ (s or p) orbit of atom α at energy E_i . The range of the summation runs over all the

TABLE II. The calculated energy differences $E_{6p}^{\text{Bi}} - E_{4p}^{\text{As}}$ and $E_{2s}^{\text{N}} - E_{4s}^{\text{As}}$ (in eV) for the different concentrations in relaxed $\text{GaAs}_{1-x}\text{Bi}_x$ and $\text{GaAs}_{1-x}\text{N}_x$ systems.

x	$E_{6p}^{\text{Bi}} - E_{4p}^{\text{As}}$	$E_{2s}^{\text{N}} - E_{4s}^{\text{As}}$
0.004	0.618	-0.832
0.031	0.662	-0.889
0.125	0.873	-0.962

valence bands of $\text{GaAs}_{1-x}\text{Bi}_x$ or all the conduction bands of $\text{GaAs}_{1-x}\text{N}_x$ alloys. We calculate the differences between E_{6p}^{Bi} and E_{4p}^{As} in $\text{GaAs}_{1-x}\text{Bi}_x$, and between E_{2s}^{N} and E_{4s}^{As} in $\text{GaAs}_{1-x}\text{N}_x$. The results for several concentrations of x are shown in Table II. We find that the E_{6p}^{Bi} is always higher than E_{4p}^{As} , and the E_{2s}^{N} is always lower than E_{4s}^{As} in all concentrations, as expected from their orbital energy differences.

Next, we analyze the wave function characters for states near the band edges for the relaxed $\text{GaAs}_{1-x}\text{Bi}_x$ and $\text{GaAs}_{1-x}\text{N}_x$ systems with different concentrations of x . For a more quantitative analysis, we define a localization factor as $\zeta = Q_{\alpha} / Q_{\text{As}}$ ($\alpha = \text{Bi}$ or N) for the same supercell calculations. Here, Q represents the normalized charge inside the muffin-tin (MT) spheres for the band-edge states. The MT radii are 1.40, 1.22, 1.64, and 0.74 Å for the Ga, As, Bi, and N, respectively. The larger the ζ value, the more localized of the state at the impurity atom site. Table III shows the calculated ζ values for the $\text{GaAs}_{1-x}\text{Bi}_x$ and $\text{GaAs}_{1-x}\text{N}_x$ alloys at the different concentrations. Figures 2(a) and 2(b) plot the charge density distributions on (110) plane of VBM and second valence band (SVB) of $\text{GaAs}_{1-x}\text{Bi}_x$ at the Γ point for $x = 0.031$ and 0.125, respectively. It is clear from these plots that, in $\text{GaAs}_{0.969}\text{Bi}_{0.031}$, the SVB state has an impuritylike charge distribution and has more charge around Bi than the VBM state. However, when the Bi concentration increases to $x = 12.5\%$, the ζ value of the VBM state is larger than that of the SVB state and the other occupied states near the band edge. So, we can conclude that at low Bi concentration, the Bi-derived impurity state is below the VBM, but at relatively high Bi concentration, the VBM of $\text{GaAs}_{1-x}\text{Bi}_x$ is mainly derived from the Bi state. Similar energy level switching has also been observed in $\text{GaAs}_{1-x}\text{N}_x$. The charge density distributions on the (110) plane of the CBM and the second conduction band (SCB) states of $\text{GaAs}_{1-x}\text{N}_x$ at Γ for $x = 0.004$ and 0.016 are plotted in Figs. 2(c) and 2(d). In Fig. 2(c) at

TABLE III. The calculated localization factor ζ of states near band edges of the $\text{GaAs}_{1-x}\text{Bi}_x$ and $\text{GaAs}_{1-x}\text{N}_x$ alloys at different concentrations. The numbers in bold highlight the ζ of the impurity derived state.

System	x	VBM	SVB
$\text{GaAs}_{1-x}\text{Bi}_x$	0.031	3.53	11.31
	0.125	3.73	2.00
$\text{GaAs}_{1-x}\text{N}_x$	0.004	4.26	5.85
	0.016	4.66	1.20

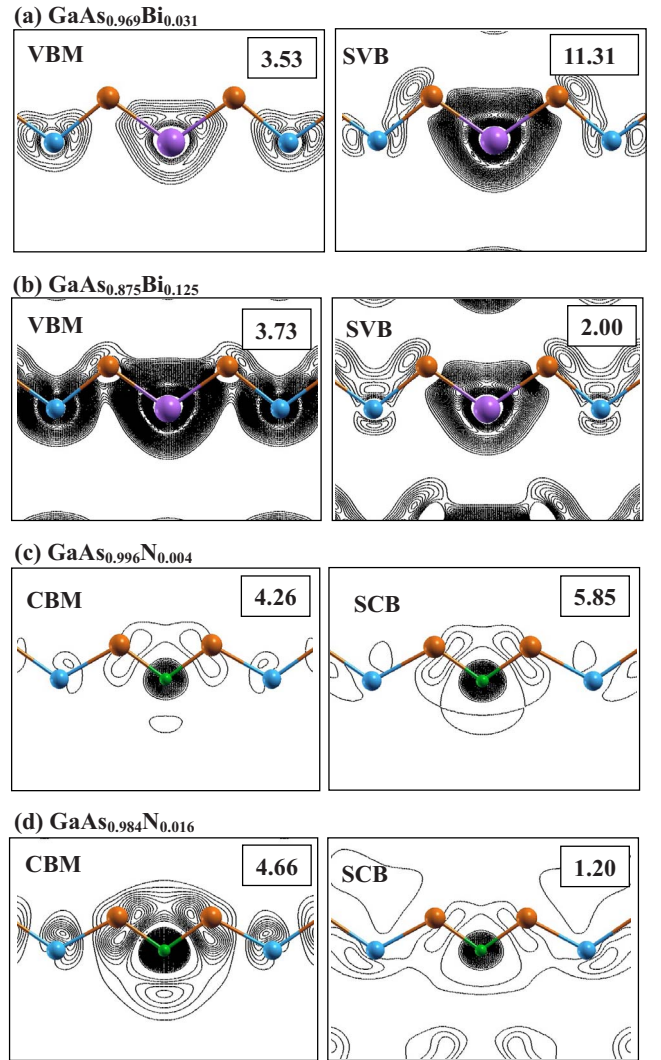


FIG. 2. (Color online) Charge density plots on the (110) plane of VBM and SVB states in $\text{GaAs}_{1-x}\text{Bi}_x$ at (a) $x = 0.031$ and (b) $x = 0.125$; of the CBM and SCB states in $\text{GaAs}_{1-x}\text{N}_x$ at (c) $x = 0.004$ and (d) $x = 0.016$. The number in each map denotes the calculated localization factor ζ value. The orange (medium gray), blue (medium small light gray), magenta (large gray), and green (small light gray) balls represent the Ga, As, Bi, and N atoms, respectively.

the very dilute concentration ($x = 0.004$), it is found that the maximal ζ value in the N MT sphere is at the SCB state. However, when the N concentration is at $x = 1.6\%$, the charge distribution of the CBM state becomes more localized at the N site. So, we can conclude that at very low N concentration, the N-derived impurity state is above the CBM, but at relatively high N concentration, the CBM of $\text{GaAs}_{1-x}\text{N}_x$ alloy is mainly derived from the N orbital.

We find that the general trends of the defect levels near the band edges of GaAs, as discussed above, can be well explained by the band broadening picture. Figure 3 shows the schematic processes of band broadening as a function of impurity concentration. The Bi 6p orbital energy is higher than the As 4p orbital energy, and the N 2s orbital energy is lower than the As 4s orbital energy. When a small amount of Bi or

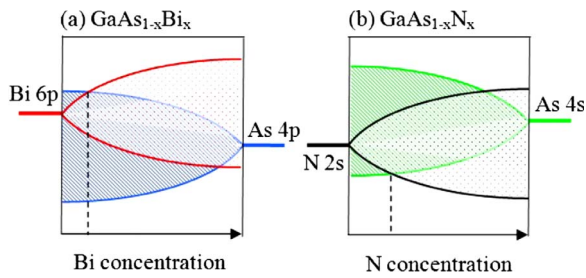


FIG. 3. (Color online) Schematic illustration of the progressions of band broadening as a function of Bi or N impurity concentration in GaAs.

N impurities are doped into GaAs, the distance between the impurity atoms is very large so the interaction between different impurity atoms will be relatively weak. Thus, the defect levels are very localized and dispersionless. However, the host atoms has strong interaction between each other, so the broadening of As 4p or 4s orbit are large. As a result, the VBM of $\text{GaAs}_{1-x}\text{Bi}_x$ and the CBM of $\text{GaAs}_{1-x}\text{N}_x$ become host-atom-derived states, and the Bi- and N-derived states are resonant inside the valence band and the conduction band, respectively (see Fig. 3). When the impurity concentration increases, the distance between impurity atoms becomes smaller, resulting in the broadening of the impurity level into a band through the strong interaction and hybridization between the impurity atoms. Therefore, as the Bi concentration increases, the broadening of the defect level Bi_{As} is able to move its top energy higher than that of As 4p band, thus becoming the VBM of the alloy [see Fig. 3(a)]. Simi-

larly, the broadening of the defect level N_{As} at higher concentration can move its lower level below the CBM of the GaAs host, thus becoming the CBM of the alloy [Fig. 3(b)].

In conclusion, based on the first-principles band-structure calculations and analysis of the electronic properties of $\text{GaAs}_{1-x}\text{Bi}_x$ and $\text{GaAs}_{1-x}\text{N}_x$ alloys as a function of alloy concentration, we show that at the impurity limit the Bi-induced impurity level is below the VBM of GaAs and the N-induced impurity level is above the CBM of GaAs, in agreement with experimental observations. However, at high concentration, the VBM of $\text{GaAs}_{1-x}\text{Bi}_x$ becomes a Bi-derived state and the CBM of $\text{GaAs}_{1-x}\text{N}_x$ becomes an N-derived state, in agreement with their chemical trends. This crossing of band characters can naturally be explained by a simple picture that takes into account band broadening and strain, but it cannot be described by the popular BAC model, indicating that the BAC model should be expanded to include not only the defect-host band interaction, but also the defect-defect and host-host interactions to give a more complete description of the band structure of the LSCM isovalent alloy systems.

This work was supported by the “973” program of the National Basic Research Program of China under Grant No. G2009CB929300 and the National Natural Science Foundation of China under Grants No. 60821061 and No. 60776061. J.L. acknowledges financial support by the “One-hundred-Talent-Plan” program of the Chinese Academy of Sciences. The work at NREL was supported by the U.S. Department of Energy, under Contract No. DE-AC36-08GO28308.

*jbl@semi.ac.cn

- ¹J. C. Woolley, in *Compound Semiconductors*, edited by R. K. Willardson and H. L. Goering (Reinhold, New York, 1962), p. 3.
- ²D. G. Thomas *et al.*, *Phys. Rev. Lett.* **15**, 857 (1965); J. J. Hopfield *et al.*, *ibid.* **17**, 312 (1966).
- ³H. P. Hjalmarson *et al.*, *Phys. Rev. Lett.* **44**, 810 (1980).
- ⁴S.-H. Wei and A. Zunger, *Phys. Rev. B* **39**, 3279 (1989).
- ⁵A. Zunger *et al.*, *Phys. Rev. Lett.* **65**, 353 (1990).
- ⁶J. Li and S.-H. Wei, *Phys. Rev. B* **73**, 041201(R) (2006).
- ⁷K. Alberi *et al.*, *Phys. Rev. B* **77**, 073202 (2008).
- ⁸W.-J. Yin *et al.*, *Phys. Rev. B* **78**, 161203 (2008).
- ⁹S.-H. Wei and A. Zunger, *Phys. Rev. Lett.* **76**, 664 (1996).
- ¹⁰J. D. Perkins *et al.*, *Phys. Rev. Lett.* **82**, 3312 (1999).
- ¹¹K. M. Yu *et al.*, *Nature Mater.* **1**, 185 (2002).
- ¹²B. Fluegel *et al.*, *Phys. Rev. Lett.* **97**, 067205 (2006).
- ¹³M. Kondow *et al.*, *IEEE J. Sel. Top. Quantum Electron.* **3**, 719 (1997).
- ¹⁴K. M. Yu *et al.*, *Phys. Rev. Lett.* **91**, 246403 (2003).
- ¹⁵B. Lee and L. W. Wang, *Appl. Phys. Lett.* **96**, 071903 (2010).
- ¹⁶J.-H. Lee *et al.*, *Phys. Rev. Lett.* **104**, 016602 (2010).
- ¹⁷J. Li *et al.*, *Phys. Rev. Lett.* **96**, 035505 (2006).
- ¹⁸A. Janotti *et al.*, *Phys. Rev. B* **65**, 115203 (2002).

- ¹⁹D. J. Wolford *et al.*, in *Proceeding of the 17th International Conference on the Physics of Semiconductors*, edited by J. D. Chadi and W. A. Harrison (Springer, New York, 1984), p. 627; P. J. Klar *et al.*, *Appl. Phys. Lett.* **76**, 3439 (2000).
- ²⁰Yong Zhang *et al.*, *Phys. Rev. B* **71**, 155201 (2005).
- ²¹J. C. Phillips, *Bonds and Bands in Semiconductors* (Academic Press, New York, 1973).
- ²²W. Shan *et al.*, *Phys. Rev. Lett.* **82**, 1221 (1999).
- ²³W. Walukiewicz *et al.*, *Phys. Rev. Lett.* **85**, 1552 (2000).
- ²⁴J. Wu *et al.*, *Semicond. Sci. Technol.* **17**, 860 (2002).
- ²⁵J. Wu *et al.*, *Phys. Rev. B* **70**, 115214 (2004).
- ²⁶K. Alberi *et al.*, *Phys. Rev. B* **75**, 045203 (2007).
- ²⁷T. Mattila *et al.*, *Phys. Rev. B* **60**, R11245 (1999).
- ²⁸Y. Zhang and A. Mascarenhas, *Phys. Rev. B* **61**, 15562 (2000).
- ²⁹P. R. C. Kent and A. Zunger, *Phys. Rev. B* **64**, 115208 (2001).
- ³⁰F. Masia *et al.*, *Phys. Rev. B* **73**, 073201 (2006).
- ³¹P. E. Blöchl, *Phys. Rev. B* **50**, 17953 (1994); G. Kresse and D. Joubert, *ibid.* **59**, 1758 (1999).
- ³²G. Kresse and J. Hafner, *Phys. Rev. B* **47**, 558 (1993); **48**, 13115 (1993); G. Kresse and D. Joubert, *Comput. Mater. Sci.* **6**, 15 (1996).
- ³³H. J. Monkhorst and J. D. Pack, *Phys. Rev. B* **13**, 5188 (1976).